Toughness of two pure block copolymer blends in high molecular weight polystyrene

O. S. Gebizlioglu*, A. S. Argon*, R. E. Cohen†
Massachusetts Institute of Technology, Cambridge, MA 02139, USA
(Received 13 February 1984)

Blends of two commercial pure block copolymers, Phillips KRO-1 and KRO-3 Resins, in high molecular weight PS were prepared by solvent casting techniques to produce composite spherical particles with two different morphologies in a majority phase of the high molecular weight PS. One type of particle had the typical KRO-1 Resin morphology of randomly wavy and often interconnected PB rods in a topologically continuous block copolymer phase of PS, while the other type of particle made of KRO-3 Resin was in the form of concentric shells of alternating layers of PB and PS block copolymer phases. Both blends were found to result in only a marginal improvement of the toughness of homo PS even for particle volume fractions as high as 0.22. This inadequate performance in the case of the KRO-1 Resin blends results from the relatively large stiffness of the KRO-1 particles, while in the case of the KRO-3 Resin blend, it results from too small an average particle size, even though the particle stiffness in the latter case is low.

(Keywords: crazing; block copolymers; composite particles; toughness; blends)

INTRODUCTION

Many glassy polymers are normally brittle in tension or any other stress state that has an important tension component. These polymers usually craze from their free surfaces. Fracture results when one such craze parts and is converted into a crack which propagates with relatively little energy absorption[1,2]. That such polymers can be toughened by controlled initiation of crazes from composite particles has been known for some time[3]. The process has been used in industry on a large scale to manufacture impact energy absorbing polymers such as high impact polystyrene (HIPS), acrylonitrile-butadiene-styrene (ABS), etc. In most of these instances, microstructures with composite particles are produced by utilizing some graft copolymers of the corresponding thermoplastic together with rubbery components to form polymeric oil-in-oil emulsions which are dispersed by various techniques in the glassy polymer phase. That the source of toughness in these materials was linked to crazes was suspected by Schmitt and Keskkula[4], who proposed that rubbery particles acted as stress concentrators to form crazes. This was directly confirmed by Bucknall and Smith[5]. Much recent research has filled in additional details of this process which has indicated: (a) that proper adhesion of the particles to the surrounding matrix was essential and could be achieved by grafting; (b) that particle sizes of a micron or larger were required to effectively initiate crazes[6]; that the particular composite nature of particles with a topologically interconnected rubbery phase containing occluded glassy polymer subparticles was of importance[7]; and that particles with random dispersal of phases inside the particles was not particularly effective[8]. Outside of the above observations many other rationalizations for achieving a tough product have been reported. Most of these, however, remain inadequately established and have not been widely supported or quantitatively justified. The possibility of achieving toughness by incorporation of stiff inclusions such as glass beads has also been tried[9,10] with marginal results. Alternatively very small compliant particles of diameters less than 0.1 μm were found to be quite effective to achieve toughness in some polymers where, however, the toughness was found to be caused by micro-shear bands initiated from these particles and involved no crazing.

It has been noted by Kawai and coworkers[11], and also by Argon *et al.*[2] that the deficient understanding of the role of particles in controlling toughness through crazing results from the difficulty of controlling the several potentially important factors such as particle chemistry, morphology, size, and overall volume fraction in commercially available material or in material produced by industrial practices. These difficulties can be overcome through the use of block copolymers and the use of ternary blending of the block copolymers with the corresponding homopolymers, to form particles of different morphology and morphological scale. Finally, such particles can then be emulsified in a majority phase of the glassy polymer of high molecular weight that is a block component of the copolymer. Although this idea is not new and has been used in part in other earlier investigations[11-16], no systematic study exists that investigates the full consequences of the particle morphology and scale on mechanical properties in a sufficiently definitive manner to draw firm conclusions. In this and the accompanying paper we present part of such a study on the use of block copolymers of PB/PS and their blends to construct composite particles in homo PS to explore this connection.

* Department of Mechanical Engineering.
† Department of Chemical Engineering.

0032-3861/85/040519-10$03.00

Table 1 Physical and mechanical properties of the materials used at 20°C

	KRO-1	KRO-3	HH-101
$\bar{M}_w$ (kg mol^{-1})	179.0	217.0	268.0
$\bar{M}_n$ (kg mol^{-1})	132.0	106.0	112.0
Density (g/cc)	1.02–1.05	1.02–1.04	1.04
Weight fraction PB	0.23	0.23	–
Yield stress (MPa)*	20.95	21.00	–
Young's Modulus (MPa)	1269.0	1474.0	3172.0
Elongation-at-break	0.09	1.10	0.02

* Craze yield stress

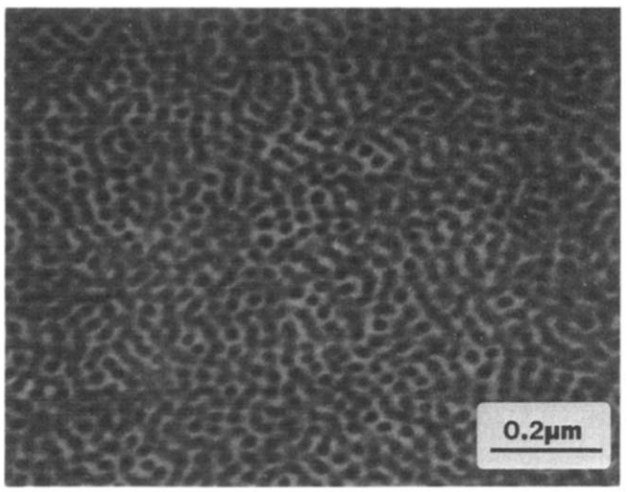

Figure 1 Microstructure of annealed KRO-1 Resin (from Argon, *et al.*[18], courtesy of J. Wiley and Sons)

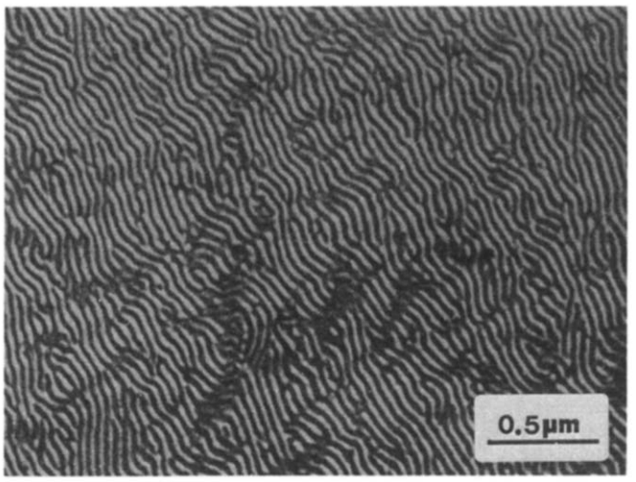

Figure 2 Microstructure of annealed KRO-3 Resin (from Argon, *et al.*[18], courtesy of J. Wiley and Sons)

EXPERIMENTAL PROCEDURE

Materials and microstructures

Two commercial polystyrene/polybutadiene (PS/PB) block copolymers made by the Phillips Petroleum Company under the designation of K-Resins and labelled as KRO-1 and KRO-3 were chosen for the basic copolymer to form particles and were blended with a heat resistant grade polystyrene of relatively large molecular weight, manufactured by Monsanto Plastics and Resins Company, and labelled as Lustrex HH-101.

The chemistry, molecular weight distribution and some mechanical properties of K-Resins have been described by Fodor *et al.*[17], a summary of which, relevant to our discussion, is given in *Table 1* which also lists the properties of the polystyrene, Lustrex HH-101.

Routine n.m.r. measurements[18] show that polybutadiene (predominantly 1,4 addition) makes up about 23% of the weight of both KRO-1 and KRO-3. Measurement by DTA-TMA reveals two distinct transitions near −90°C and 95°C for K-Resins corresponding to PB and PS, respectively.

Transmission electron microscopy has shown two radically different microstructures for K-Resins. The KRO-1 Resin has a morphology that consists of randomly wavy and often interconnected rods of PB, shown in *Figure 1*. The microstructure of KRO-3 Resin consists of lamellae of PB with 20 nm thickness and large aspect ratio, which range in packing from regularly aligned lamellar domains with randomly varying misorientation in the annealed material, shown in *Figure 2*, to randomly corrugated and wavy sheets in the as-received material. The matrix polymer is a polystyrene which is commercially used for biaxially oriented film and foam sheet extrusion applications. The sample provided by the Monsanto Plastics and Resins Company contains no additives other than a molecularly dissolvable tinting agent at a composition of 0.16% by weight. This PS was particularly chosen to be of considerably larger $\bar{M}_w$ than the $\bar{M}_w$ of the polystyrene in the block component of the block copolymer to achieve the desired incompatibility that results in the rejection of the block copolymer phase in particulate form in the polystyrene. All the mechanical properties data given in *Table 1* have been obtained according to the ASTM Test Method D638.

Film preparation

All microstructural examinations and mechanical properties tests have been conducted on films of thickness 0.5–0.7 mm. The film preparation starts with dissolving weighed quantities of either KRO-1 or KRO-3 Resin and polystyrene HH-101 in 100 ml of reagent grade toluene which is a good solvent for both. Typically, 5 g of polymer of varying KRO-1 or KRO-3 content are dissolved and left overnight for complete dissolution in a flask. The flask is occasionally shaken but not mechanically stirred. The solution is fed through a Millipore Teflon filter of 10 μm pore size and is then fed into a spin cup made of aluminium and spinning at 3600 rpm to cast a thin annular film. Mylar is used as a lining of the spin cup, to give a smooth film surface. The spin caster is kept in an environmental chamber which provides close temperature control to as high as 100°C–150°C. An inert atmosphere is maintained in the chamber by a constant inflow of dry nitrogen gas from a cylinder through a gas rotameter to control the gas flow rate. The spin casting is followed by annealing at 100°C in a vacuum oven, maintaining a pressure of 3×10^{-3} torr. Further details of the spin caster and its use have been described elsewhere[19].

Microscopy

The microstructures of dispersions of K-Resins in polystyrene were examined in a Phillips 200 transmission

electron microscope, which is operated at an accelerating voltage of 80 KV. A small piece cut from the cast film was stained with a 1% (by weight) aqueous solution of OsO_4.[20] This technique is commonly used to accentuate the phase contrast in systems containing an olefinic component by attaching an osmium atom on the olefinic component. This enhances the electron absorption in the rubbery phase and provides good contrast against polystyrene that remains largely transparent to the electron beams. Sections of thickness in the range of 500–900 Å were cut from such stained specimens by means of an LKB 8800 Ultramicrotome III, using glass knives.

For the examination of craze microstructures, the specimens were crazed first in an Instron Tensile Tester, then transferred to a 'hand crazing' device, and held extended by the clamps of this device. In order to prevent craze recovery and alteration of the craze microstructure during the long periods of fixing, the OsO_4 staining is carried out by immersing the stretched specimens in a 1% solution of OsO_4 in water for a few days. The cuts in the ultramicrotome, are made in a direction approximately 45° to the principal tensile axis. The sections are taken across the thickness of the specimen, at right angles to the craze planes to produce the minimum number of artifacts on the craze microstructure. Stereological measurements of the particles in the micrographs were made with a Magiscan Image Analyzing Computer, manufactured by Joyce–Loebl.

Light microscopy was routinely performed for the examination of specimen surface features and development of craze packets by means of a Zeiss Ultraphot II Microscope.

Tensile testing

All tensile tests were performed on an Instron Tensile Testing Machine Model 1122. Standard specimens with reduced gauge lengths were cut from spin-cast films varying in thickness from 0.5 mm to 0.7 mm between batches. The gauge length of specimens was 6.35 mm, with a width of 3.18 mm. Prior to testing, all specimens were conditioned in the standard laboratory atmosphere of 23°C and 55–60% relative humidity for at least a day. The majority of tensile tests were conducted at a strain rate of $1.3 \times 10^{-4}\ s^{-1}$. Some tests were also performed at speeds as high as $10.84\ s^{-1}$ with the use of specially prepared grips and an Instron Servo-hydraulic Machine Model 1331.

EXPERIMENTAL RESULTS

Morphology control

Several degrees of freedom are available for obtaining composite particles with different morphologies and at different volume fractions by emulsification of block copolymers in high molecular weight polystyrene. In a most direct way block copolymers with a given morphology can be used in emulsions in high molecular weight PS to form composite particles having the same morphology as the bulk block copolymer[21,22]. The size, size distribution and shape of such particles, however, are strongly dependent on the condition and techniques of preparation. Thus, Cohen and Bates[23] demonstrated a great sensitivity of block copolymer morphologies to the rate of solvent evaporation in film casting. Rapid casts give non-equilibrium morphologies that exhibit relatively large regions of material embedded in the microphase separated block copolymer while slow cast films show highly regular and well-defined micro-structures.

For its simplicity, reproducibility, speed and overall quality of the films, solution blending was used throughout the course of this investigation to prepare charges for spin casting. An exploratory study of film preparation was conducted to determine optimum casting conditions, thermal treatments, and film characteristics. As a result a blend composition of 21.7% by weight of block copolymer KRO-1 or KRO-3 was chosen. This corresponds to a rubber (polybutadiene) composition of 5% in the blend which is close to what is usually used in commercial HIPS.

Conditions of spin casting

In preliminary experiments on the selection of an optimum schedule for spin casting to achieve a relatively uniform distribution of composite particles with an acceptable size range much variation was found in the distribution of the block copolymer phase in the majority phase of the Lustrex HH-101 PS. Thus, in one step casts of the solutions of K-Resins and HH-101 PS in toluene at temperatures of 23°C, 40°C and 70°C, objectionable phase separation of the K-Resin into a surface layer was found. Clearly under these conditions effective centrifugal separation of phases occurred. Since in all these one step casts complete solvent removal was demanded, the casting times were progressively shorter as the temperature increased. In all cases a dry nitrogen flow rate of 0.24 litres min^{-1} was maintained through the chamber containing the spin caster. To overcome the objectionable phase separation two stage casting schedules were tried in which partial solvent removal at relatively low temperatures was accomplished while the solution was sufficiently viscous to inhibit the centrifugal separation, followed by a higher temperature excursion to finish the solvent removal. Thus, the best procedure that was found to obtain the microstructures reported here consisted of an initial period of 66 h at 40°C followed by a finishing step at 100°C for 24 h. This resulted in almost completely solvent-free films with enough mechanical integrity to be removed from the drum of the spin caster. All films were then given a static annealing treatment at 100°C for another 24 h in a vacuum oven to equilibrate the microstructure, remove any residual interphase stresses due to the centrifugal forces, and finally to remove any remaining traces of solvents. Since a net weight loss of 0.5–0.7% occurred during this final vacuum annealing step it is evident that the two step spin casting had not fully removed all solvents in the films. Films were oven cooled at a rate of approximately 10°C per hour. This is fast enough to prevent very extensive physical ageing and slow enough to prevent development of thermal stresses due to rapid cooling. The final films varied in thickness between 0.5–0.7 mm from batch to batch but were quite uniform in thickness in any one cast, and were of high quality and with smooth surfaces. Transmission electron microscopy of the films prepared according to the above mentioned schedule revealed a relatively uniform distribution of composite particle phases of KRO-1 and KRO-3 Resin with relatively wide particle size distributions that will be

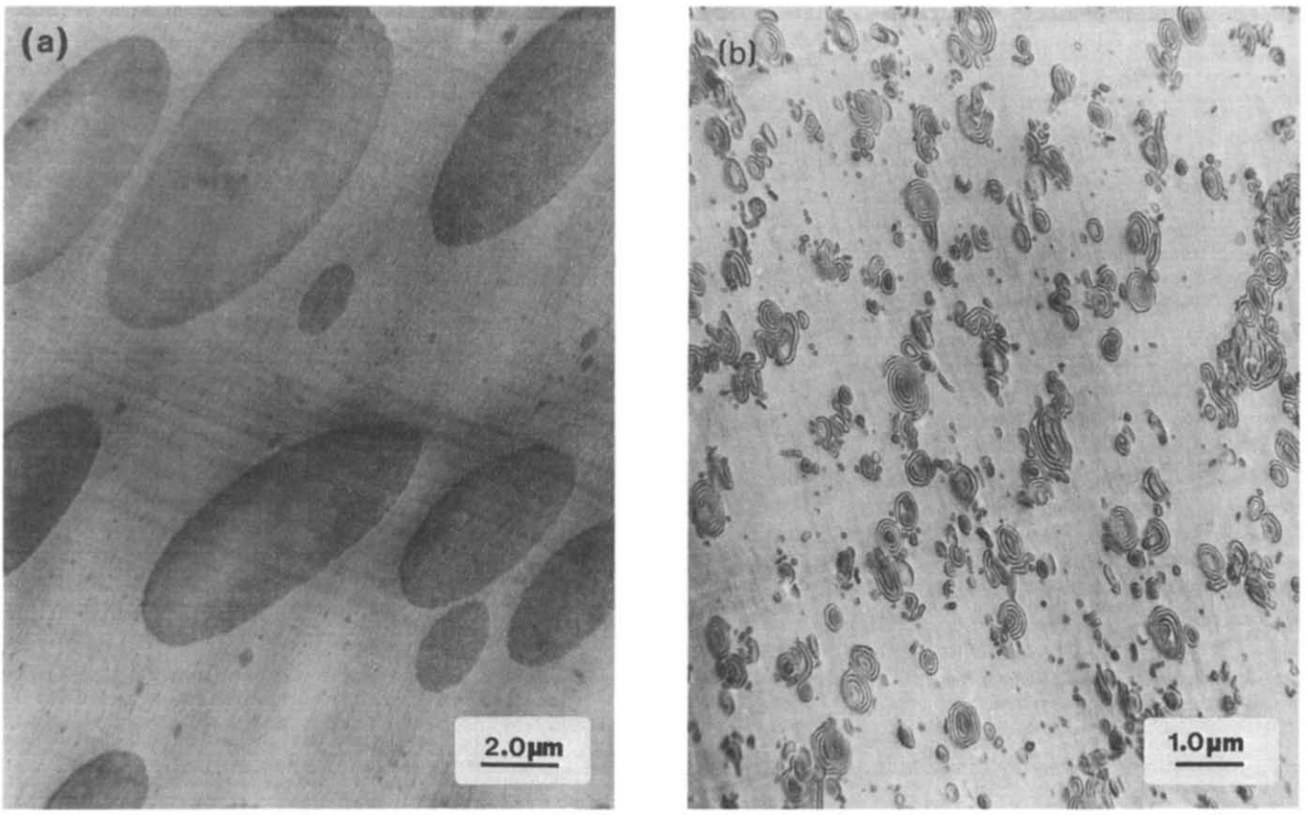

Figure 3 Microstructure of the two K-Resin blends in high molecular weight PS: (a) particles of KRO-1 Resin morphology in the blend with KRO-1 Resin; (b) particles with a morphology of concentric spherical or cylindrical layers of PS and PB in the blend with KRO-3 Resin

discussed in detail below. As *Figures 3a* and *3b* show, the average sizes were much larger for the KRO-1 Resin particles than for the KRO-3 Resin particles. The morphology of the KRO-1 particle is identical to the KRO-1 block copolymer phase in isolation, while that of the KRO-3 particles appears to be concentric spherical (or cylindrical) layers of the block copolymer enclosing a substantial central inclusion of PS that might be incorporating some of the low molecular weight fraction of the HH-101 PS *Figures 4a* and *4b*. All particles observed in such micrographs show elliptical sections with their minor axes parallel to the direction of microtoming. On the basis of this, it is suggested that the actual particles in the un-cut blend are probably of spherical shape and have been distorted into oblate spheroids during the cutting operation.

Stereology of the particulate phase

The particle volume fractions in the micrographs are determined by areal analysis, where the uncertainty or statistical error will depend on the number of features in the sub-area of a given section. For a uniform distribution of the second phase particles the number N of the sectioned particles appearing within the sub-area will follow a Poisson frequency function[24]. Consequently, the variance $\sigma^2(N)$ in the numbers N will just be equal to the expected or average value $\bar{N}$ of N, where $\sigma(N)$ is the standard deviation of the many samplings of sub-areas. This gives a relationship of:

$$\sigma^2(N)/(\bar{N})^2 = 1/\bar{N} \tag{1}$$

However, the variability in the size of the features must also be taken into account. Then it is possible to place the following lower limit on the variance of an areal analysis that represents the relative error,

$$\frac{\sigma(\bar{c}_v)}{\bar{c}_v} \geqslant \frac{1.1}{\sqrt{N}} \tag{2}$$

where $\bar{c}_v$ is the average volume fraction of the spherical inclusion phase. In order to get a relative error of less than 5%, it is necessary to measure the areas of about 500 particles on the plane of cut. In our analyses, all the measurements were made on a particle population of 1000 to 1200, thereby reducing the relative error to 3%. The average area fraction of the particulate phase has to be corrected for the bias arising from failure to observe a true opaque planar section when transmitted illumination is used (the so-called Holmes effect). An adequate correction for this is provided by the expression[25]

$$A_c = \bar{A}(2\bar{D}/(2\bar{D} + 3t)) \tag{3}$$

where
A_c = corrected area fraction
$\bar{A}$ = average area fraction
$\bar{D}$ = average particle diameter
t = thickness of section

which is valid for thin sections where no particle overlap can occur[25].

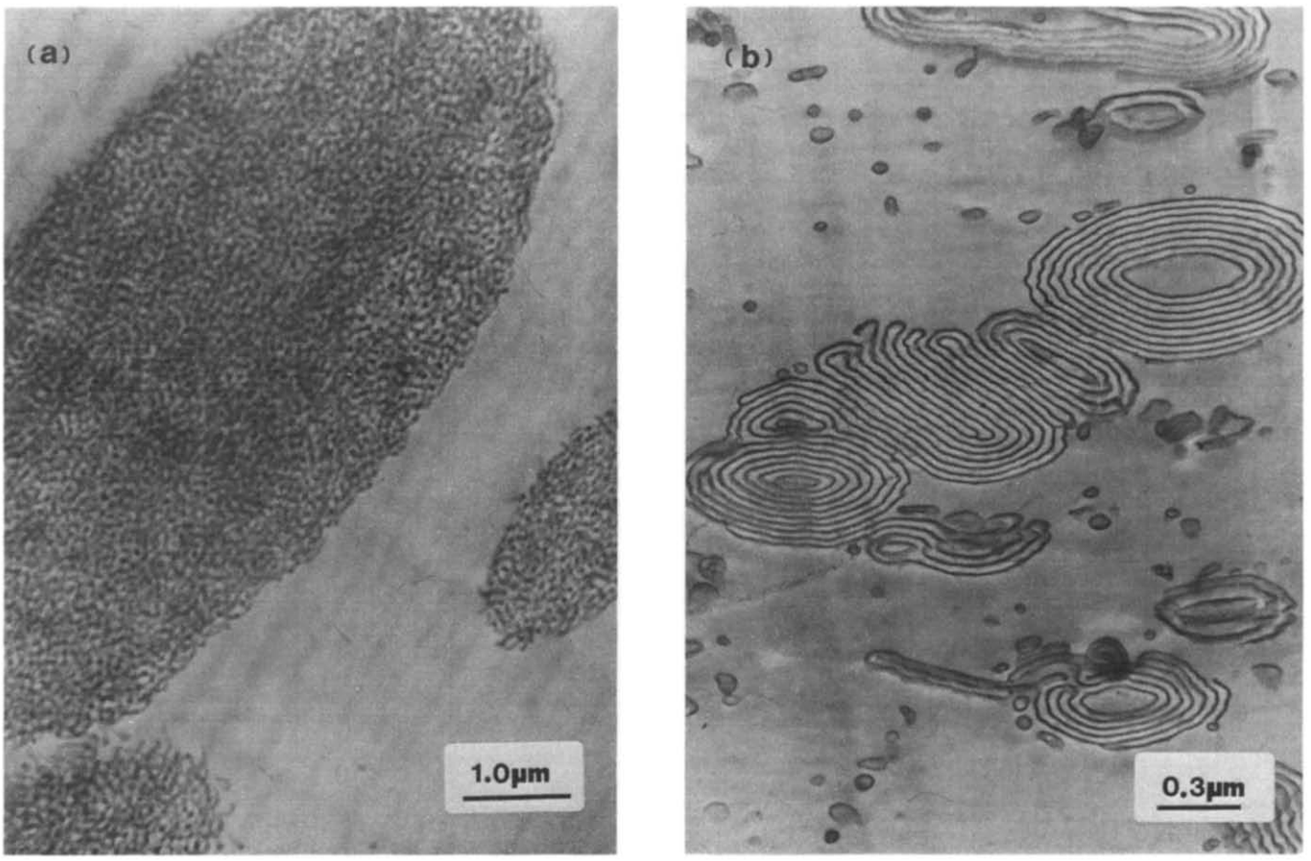

Figure 4 Micrographs showing the internal detail of composite particles in the two K-Resin blends; (a) particles with the KRO-1 morphology; (b) particles with a morphology of concentric shells in the KRO-3 blend

The histograms of particle areas as observed in TEM micrographs for the two main blends of KRO-1 and KRO-3 Resins, both at a weight fraction of 0.22 in HH-101 PS are shown in *Figures 5a* and *5b*. Inspection of these distributions shows that the minimum particle areas of the two distributions are rather similar at a level of 10^{-15} m^2 which is of individual block dimensions of the block copolymers indicating that a small fraction of the block copolymer remains unassociated in the PS matrix. Apart from this expected feature the distribution of particle areas is much broader for KRO-1 Resin particles, reaching up to particles with areas as large as 3.2×10^{-11} m^2, while the largest KRO-3 particle in the distribution is only 7.4×10^{-12} m^2. Considering all corrections it is found that for the KRO-1 Resin blend the number average particle diameter is 0.83 μm with a number density of particles in a random section of 5.186×10^{11} particles per m^2. In the corresponding case of the KRO-3 blend the number average particle diameter is only 0.39 μm with a number density in a random section of 2.35×10^{12} particles per m^2. These average sizes have been corrected for a typical section thickness of 70–80 nm in the microtome sections.

Blends with different volume fractions of K-Resin

In addition to the principal composition of a 0.217 fraction of K-Resin in PS for both KRO-1 and KRO-3 several additional blends were also prepared with different compositions of KRO-1 Resin. The preparation techniques of these blends were identical to those of the principal composition. *Table 2* shows these blends that consisted of weight fraction of KRO-1 Resin of 0.01, 0.05 and 0.435 in addition to the principal composition of 0.217. The stereological results in the last three columns of *Table 2* indicate a relatively constant number density of particles per unit volume and a monotonic increase in average (spherical) particle diameter with increase of volume fraction of particulate phase. This suggests a problem of heterogeneous nucleation of particles from a relatively constant volume density of embryos. The source of this effect is not clear, but it could be related to an inadvertant particulate component of impurity that has not been filtered out.

The particle area distributions for the blends with weight fraction of KRO-1 of 0.01, 0.05 are given by the histograms in *Figures 6a* and *6b*. Once again the histograms show a broad distribution of particle sizes ranging all the way from small clusters of individual blocks of copolymer to dimensions in excess of 8.3 μm for the most concentrated blends. In all cases an undesirable monotonic increase of particle size with particle volume fraction (at roughly a constant number density of particles) was found, while what was clearly desirable was a constant particle size with decreasing average particle spacing as volume fraction of particles increases. How this can be achieved, at least partially, by a special schedule of pre-

concentration of solution before casting will be the subject of a separate paper.

Tensile tests

Figure 7 summarizes the tensile test results for the typical behaviour of all the blends containing KRO-1 Resin and the blend containing KRO-3 Resin at a conventional strain rate of $1.3 \times 10^{-4}\ s^{-1}$. The Figure shows that the yield stress and the modulus monotonically decrease with increasing volume fraction of KRO-1 Resin in the blends. This trend is also accompanied with a modest monotonic increase in the strain to fracture. When compared with the behaviour of the unblended PS, however, the changed behaviour of the KRO-1 Resin blends is disappointingly little and not commensurate with the relatively large volume fraction of the K-Resin incorporated. The effect of incorporation of KRO-3 Resin is considerably larger in the Young's modulus and yield stress. Both are decreased by nearly 40% with incorporation of a volume fraction of 0.217 of KRO-3 Resin. The increase in the strain to fracture, however, is almost the same as that for the corresponding blend with KRO-1 Resin. The trends shown in *Figure 7* are qualitatively in agreement with expectations on the basis of the different morphologies of the two types of particles. In the randomly intermixed phase morphology of KRO-1 Resin there exists a topologically continuous block component of PS that results in a particle stiffness close to the upper bound estimate for this composition of phases. On the other hand the concentric shell morphology of phases in the KRO-3 particle disrupts the topological continuity of the majority phase of PS in these particles and gives them a low stiffness that must be closer to a lower bound estimate for the same volume fraction of phases of PS and PB.

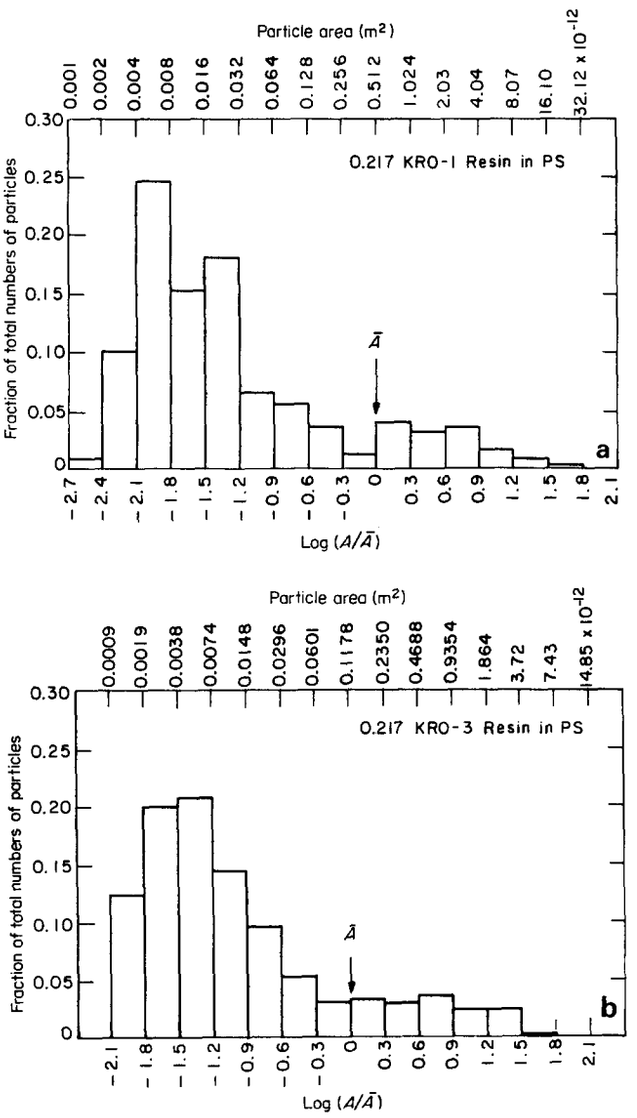

Figure 5 Histograms of the size distribution of particle cross-sectional areas in the two main blends of 0.217 volume fraction of K-Resin in high molecular weight PS; (a) particle area distribution in the KRO-1 Resin blend; (b) particle area distribution in the KRO-3 Resin blend

Figure 8 shows the comparative results of the effect of two very different strain rates in the tests for a 0.217 KRO-1 Resin blend. An increase in the strain rate from $3.3 \times 10^{-3}\ s^{-1}$ to $2.17\ s^{-1}$ results in a negligible change in Young's modulus and only a 12% rise in the yield stress.

Craze distribution

Visual examination of the specimens in the tensile apparatus during deformation and light microscopy of partially deformed specimens has established that whitening in all the blends initiates primarily at surface imperfections along the cut edges of the specimens. Typical cases for KRO-1 and KRO-3 blends are shown in *Figures 9a* and *9b*. These Figures show that the whitening zones in KRO-1 blends are relatively planar and arrange themselves nearly perpendicular to the applied stress. In KRO-3 blends the whitening zones are much wavier and fragmented. No significant transverse contractions are found in the whitened specimens, indicating that the plastic strains recorded are almost completely dilatational. Although the volume fraction of K-Resins incorporated in these blends is relative small (i.e. of the order of 0.217) and the majority phase is a common topologically continuous high molecular weight of PS in both cases, the distribution of the whitening described above is very similar to the whitening reported by Argon

Table 2 Blends of KRO–1 in polystyrene

KRO–1 in the blend Weight fraction	Volume fraction	Weight fraction PB	Particle volume fraction	Number density particles, m^{-2}	$\bar{D}_{eq}$ (μm)
0.01	0.010	0.002	0.011	9.203×11^{11}	0.16
0.05	0.051	0.011	0.053	10.786×10^{11}	0.32
0.217	0.220	0.050	0.235	5.186×10^{11}	0.83
0.435	0.440	0.100	0.458		

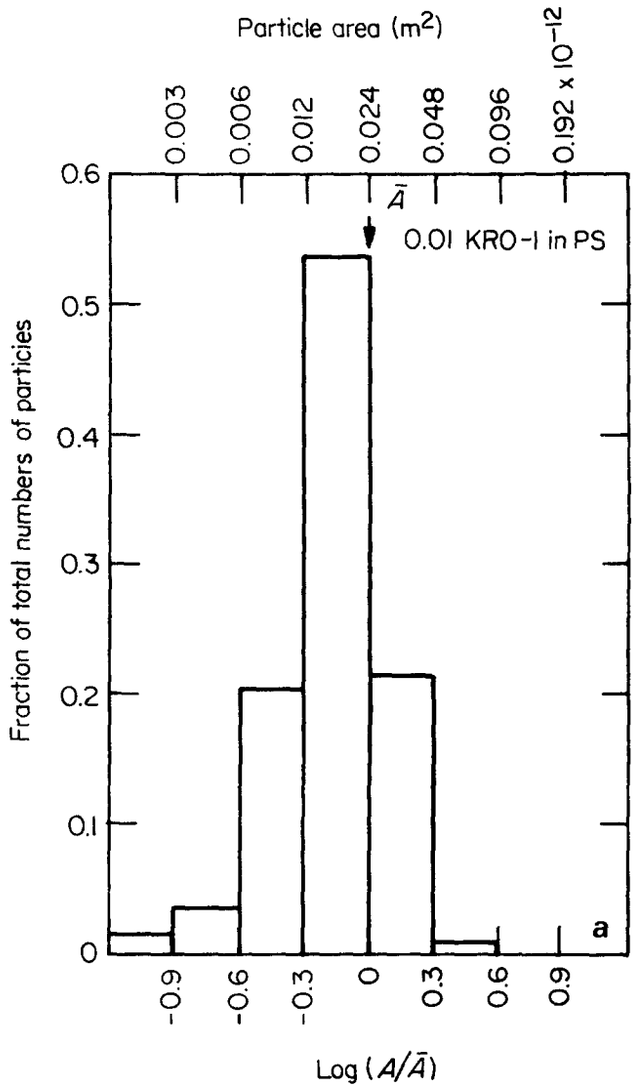

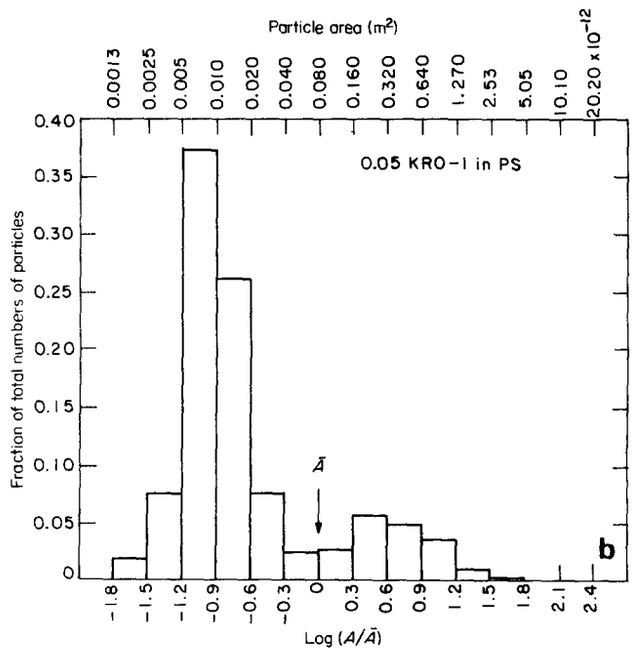

Figure 6 Particle size distributions in the TEM micrographs of two other KRO-1 Resin blends with: (a) a volume fraction of 0.01 KRO-1 in PS: (b) a volume fraction of 0.05 KRO-1 in PS

et al.[18] in the tensile experiments on pure KRO-1 and KRO-3.

Fracture occurs finally by the development of a crack at the centre of one of the most intense whitening zones from the edge of the sample and propagates across the specimen by a ductile tearing mode. Under the typical straining rates of $1.3 \times 10^{-4}\ s^{-1}$, fracture by tearing is completed in the KRO-1 blends within about one second, while the same process along a more jagged path takes on the order of about 5 s in the KRO-3 blend. *Figure 10* shows a stably advancing ductile tearing crack in a KRO-3 Resin blend. This difference in tearing behaviour is most likely a result of the significant differences in stiffness and flow stress between the two blends. The observations emphasize, however, the importance of surface imperfections in both governing the sites from which plastic deformation by whitening (cavitation or crazing) initiates as well as the sites at which eventual fracture begins.

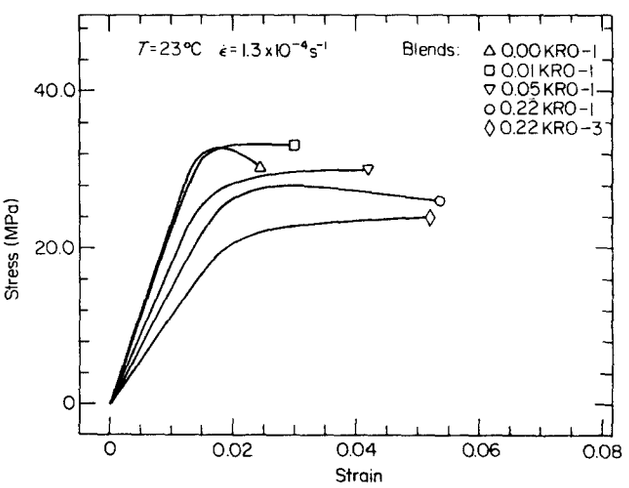

Figure 7 Typical stress–strain behaviour of the cast and annealed films of three of the KRO-1 blends and the KRO-3 blend strained at room temperature and at a strain rate of $1.3 \times 10^{-4}\ s^{-1}$

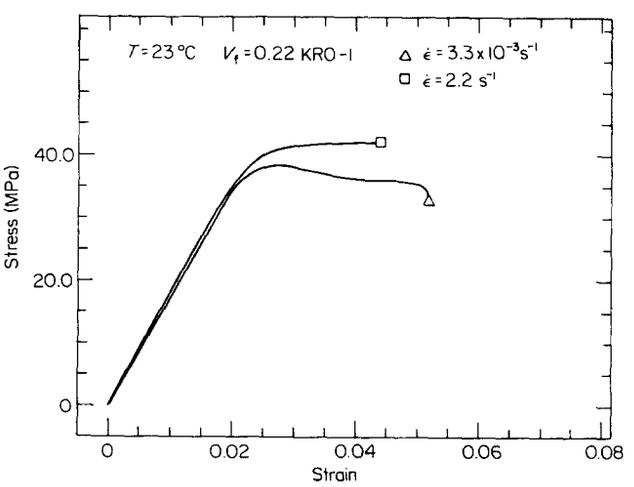

Figure 8 Stress–strain behaviour of a KRO-1 blend with a volume fraction of KRO-1 Resin of 0.22 at two different strain rates

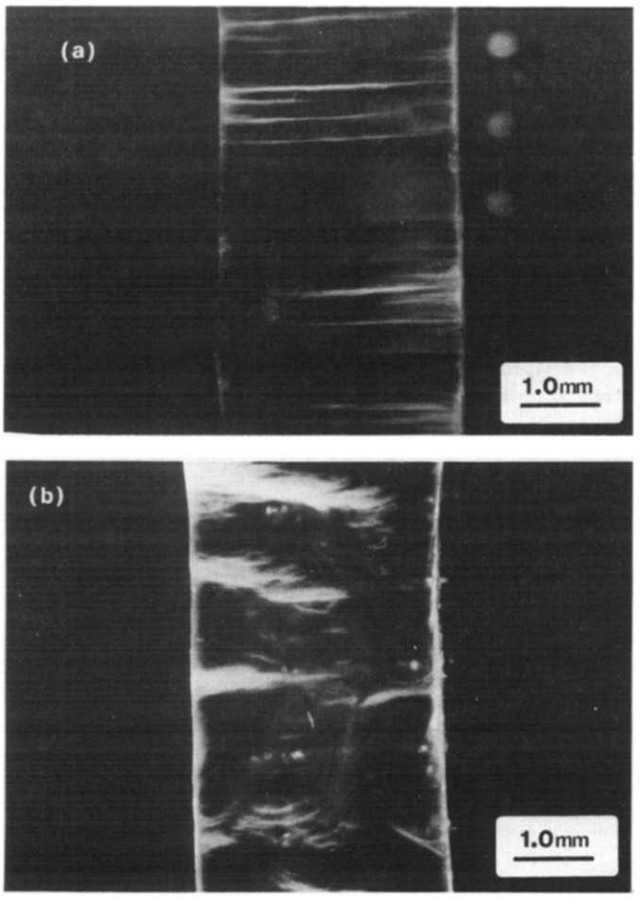

Figure 9 Distribution of whitening through crazing in the two main blends of K-Resins with volume fractions of 0.22 of resin; (a) KRO-1 blend; (b) KRO-3 blend

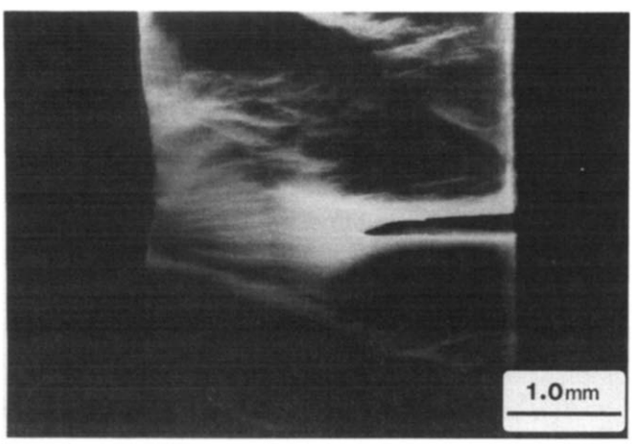

Figure 10 Propagation of a tearing crack in a KRO-3 Resin blend

Craze morphology

Transmission electron micrographs of crazes in the various blends have shown little evidence for craze initiation from KRO-1 particles. *Figure 11* shows the morphology of a typical craze in a KRO-1 Resin blend. It has the same internal detail of drawn fibres and a terminal thickness of about 0.2 μm. The micrograph shows the craze to go through a particle. *Figure 12* shows a more complex case of craze interaction with composite KRO-1 Resin particle. Here again the taper angle of the crazes suggests that the craze has arrived at the particle and is being arrested or diverted by it rather than being initiated by the particle. It is clear that the interwoven PB rod morphology of the KRO-1 particle makes it an effective craze arresting medium without introducting large voids into the craze fibril structure that can act as a defect to initiate craze fracture. The low efficiency of particles with this morphology is no doubt due to the topologically continuous PS phase inside the particle that gives it a high stiffness and results in too small a stress concentration around the particle that is insufficient to initiate crazes. That this must be the case had already been pointed out

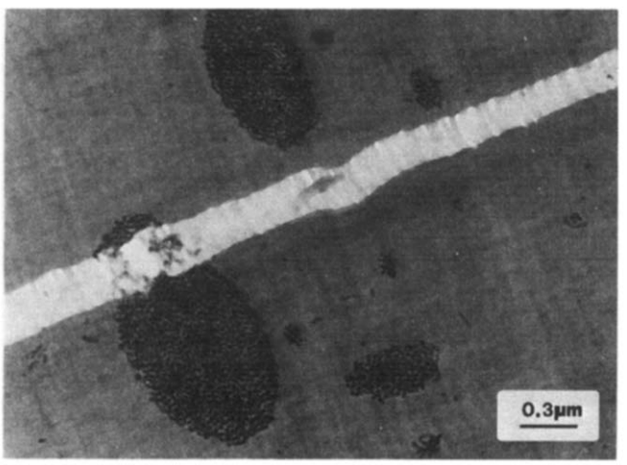

Figure 11 Micrograph of a straight craze in a KRO-1 Resin blend showing the typical craze microstructure of PS. The craze has consumed a particle in its path

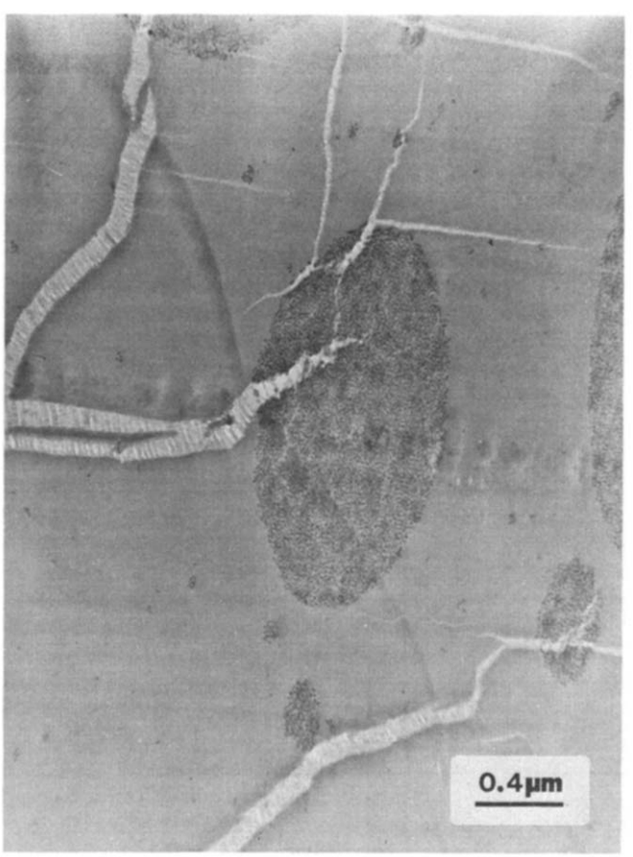

Figure 12 Diversion of crazes by particles in a KRO-1 blend

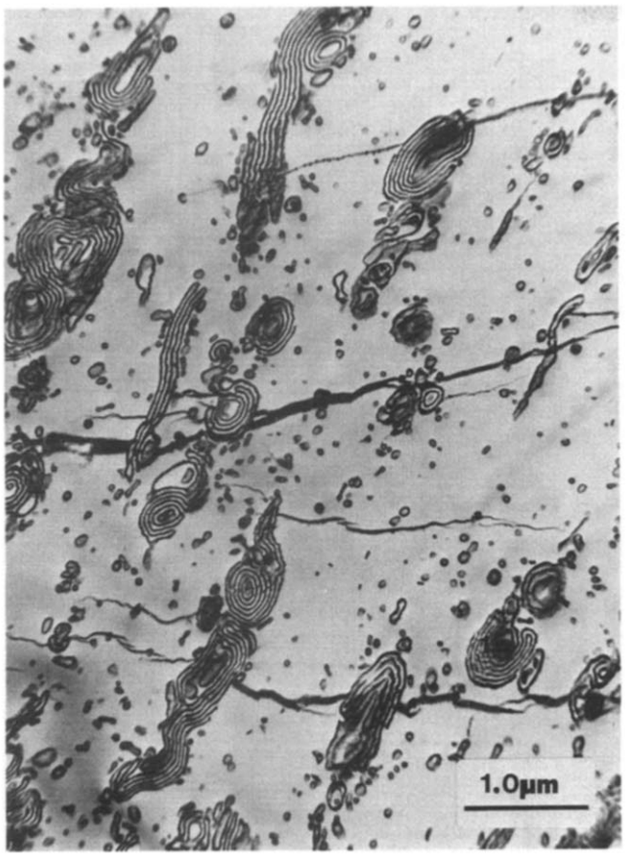

Figure 13 Micrograph of crazes in a KRO-3 Resin blend, showing very wavy crazes with an inverted electron image contrast. Some interaction of crazes with particles, particularly in their pole regions is observed

by Argon *et al.*[8] in the course of a study of a special type of particle modified PS containing particles with several different morphologies.

Figure 13 shows crazes in a KRO-3 Resin blend where some evidence of strong craze interaction at the poles of some particles is observable. Examination of a large number of different areas in the microtomed samples has established that the crazes in the KRO-3 blends are usually much wavier than those in KRO-1 blends. This is most likely a direct result of the larger number density of particles with a smaller average size, and a size distribution favouring small particles. Since the KRO-3 particles are also much more compliant than the KRO-1 particles, crazes growing in the majority phase of PS must be subjected to stronger perturbations of local stress than is the case in KRO-1 Resin blends. Examination shows furthermore, that while the morphology and electron image contrast of the crazes in PS of the KRO-1 blends look very much like those in homo-PS, those in the KRO-3 blend are thinner and have in large part an inverted electron image contrast, i.e. the crazes appear black on light background of solid PS in the KRO-3 blends. While the smaller thickness of the crazes in the KRO-3 blends may also be a result of the enhanced perturbation of the craze with the many small particles, the explanation of the inverted electron image contrast of the craze matter is not clear.

DISCUSSION

We have presented a study of the craze initiating efficiency and overall toughening effect of two very different particle morphologies in high molecular weight PS. The results have shown that it is possible to incorporate block copolymer phases in homo-PS by solvent casting techniques. In the special solvent extraction schedule used in this study where the dilute solution of the copolymer with the high molecular weight homo-PS is introduced into the spin caster and the solvent is removed first for 66 h at 40°C and then for 24 h at 100°C, wide particle size distributions are obtained and the average particle size is not separately controllable from the volume fraction of the particulate component. Better particle size control is possible through the adoption of a technique of Turley and Keskkula[26] where static solution concentration is achieved first resulting in the formation of large islands of block copolymer by coagulation. A desired particle size is then achieved by a controlled amount of stirring to break up the coagulant phase before introduction into the spin caster. The results of such a study will be reported elsewhere[27]. Nevertheless, in spite of the rather wide size distribution of the particles and a large difference in the average sizes of the particles of the KRO-1 and KRO-3 resins in the blends, two very different particle morphologies have been obtained.

The particles in the KRO-1 Resin blends retain the characteristic KRO-1 Resin morphology which is made up of a randomly wavy, and often interconnected rod shaped PB domain surrounded by a topologically continuous domain of PS. Clearly in this morphology the stiffness of the particle is high and must be very close to that which is given by an upper bound estimate. Hence, the concentration of stresses around the particles will be relatively small and large applied stresses are necessary to initiate crazes from the interfaces of the particle. Experiments show that under these conditions surface stress concentrations are more effective craze initiation sites and the particles act primarily as arrest sites of crazes or to divert crazes. Since the required craze flow stresses are high, and of the order of what is encountered in homopolystyrene, craze matter is subjected to large stresses and early breakdown occurs preferentially from the same surface discontinuities that have initiated the crazing. Fracture follows before much additional dilatational flow can be initiated from other surface discontinuities with lesser stress concentration. The overall strain to fracture is little, resulting in low levels of toughness. These results confirm the similar earlier conclusions of Argon *et al.*[8] in a study of PS with multi-morphology particles, that the particles with randomly dispersed phases having a topologically continuous PS phase are much less effective in initiating crazes than the conventional HIPS particles which for the same volume fraction of a PB phase have this phase as the topologically continuous one resulting in considerably lower particle stiffness and a higher efficiency of craze nucleation. It is appropriate to note here that the perturbation on the overall stress concentration produced by the PB phase in the KRO-1 Resin morphology is of too small a wave length to initiate crazes.

The particles in the KRO-3 Resin blends have a concentric spherical or cylindrical shell morphology which imparts to these composite particles a relatively low radial stiffness[28] that should make them efficient nucleators of crazes, as we have demonstrated in the

accompanying study[29]. In the present study, however, the KRO-3 Resin blend is only very marginally better than the KRO-1 Resin blends. This disappointing result is most likely due to the narrower overall particle size distribution that has a large fraction in the very small particle range giving an average particle diameter of only 0.42 μm that is clearly too small for initiation of crazes in the highly stressed equatorial regions of the particles. Thus, if for the same volume fraction of particles the average particle size could be increased to the range of 1–2 μm the concentric shell morphology of particles should prove to be very effective in nucleating crazes. That this is indeed so has been demonstrated in the accompanying study[29].

ACKNOWLEDGEMENT

This research was supported by the NSF-MRL Program through the Center for Materials Science and Engineering at M.I.T. under Grant No. DMR 81-19295. It also received support in the form of a post-doctoral fellowship (for O. S. Gebizlioglu), made possible through the generous help of the Monsanto Polymer Products Company of Springfield, Massachusetts for which we are particularly grateful. We acknowledge also with thanks the many stimulating discussions we have had with Dr F. S. Bates, and Mr C. E. Schwier.

REFERENCES

1 Kramer, E. J. in 'Advances in Polymer Science: Crazing', (Ed. H. H. Kausch), Springer, Berlin, Vol. 52/53, p. 1 (1983)
2 Argon, A. S., Cohen, R. E., Gebizlioglu, O. S. and Schwier, C. in 'Advances in Polymer Science: Crazing in Polymers', (Ed. H. H. Kausch), Springer, Berlin, Vols. 52/53, p. 275 (1983)
3 Bucknall, C. B. 'Toughened Plastics', Appl. Sci. Publ., London (1977)
4 Schmitt, J. A. and Keskkula, H. *J. Appl. Polym. Sci.* 1960, **3**, 132
5 Bucknall, C. B. and Smith, R. R. *Polymer* 1965, **6**, 437
6 Bucknall, C. B. *J. Mater. Sci.* 1969, **4**, 214
7 Silberberg, J. and Han, C. D. *J. Appl. Polym. Sci.* 1978, **22**, 599
8 Argon, A. S., Cohen, R. E., Jang, B. Z. and VanderSande, J. B. in 'Toughened Plastics', Plastics and Rubber Inst., London, pp. 16–1 (1978)
9 Sahu, S. and Broutman, L. *J. Mater. Sci.* 1971, **8**, 98
10 Lavengood, R. E., Nicolais, L. and Narkis, M. *J. Appl. Polym. Sci.* 1973, **17**, 1173
11 Kawai, H., Hashimoto, T., Miyoshi, K., Uno, H. and Fujimura, M. *J. Macromol. Sci.-Phys.* 1980, **B17**, 427
12 Craig, T. O. *J. Polym. Sci. Polym. Chem. Edn.* 1974, **12**, 2105
13 Riess, G., Marti, S., Refregier, J. L. and Schlienger, M. in 'Polymer Alloys', (Eds. D. Klempner and K. C. Frisch), Plenum Press, New York, p. 327 (1977)
14 Echte, A. *Angew. Makromol. Chem.* 1977, **58/59**, 175
15 Eastmond, G. C. and Phillips, D. G. in 'Polymer Alloys', (Eds. D. Klempner and K. C. Frisch), Plenum Press, New York, p. 147 (1977)
16 Kruse, R. *ACS Polym. Prepr.* 1977, **18**(1), 838
17 Fodor, L. M., Kitchen, A. G. and Biard, C. C. *ACS Organ. Coat. and Plast. Chem. Prepr.* 1974, **34**(1), 130
18 Argon, A. S., Cohen, R. E., Jang, B. Z. and VanderSande, J. B. *J. Polym. Sci. Polym. Phys. Edn.* 1981, **19**, 253
19 Bates, F. S., Cohen, R. E. and Argon, A. S. *Macromolecules* 1983, **16**, 1108
20 Kato, K. *Polym. Eng. Sci.* 1967, **7**, 38
21 Gebizlioglu, O. S., Argon, A. S. and Cohen, R. E. *ACS Polym. Prepr.* 1981, **22**(2), 257
22 Gebizlioglu, O. S., Argon, A. S. and Cohen, R. E. *SPE-Tech. Papers* 1982, **28**, 126
23 Cohen, R. E. and Bates, F. S. *J. Polym. Sci. Polym. Phys. Edn.* 1980, **18**, 2143
24 Hilliard, J. E. in 'Quantitative Microscopy', (Eds. R. T. DeHoff and F. N. Rhines), McGraw-Hill, New York, p. 46 (1968)
25 Underwood, E. E. 'Quantitative Stereology', Addison-Wesley, Reading, Mass., p. 103 (1970)
26 Turley, S. G. and Keskkula, H. *Polymer* 1980, **21**, 466
27 Gebizlioglu, O. S. and Sun, S-T., to be published
28 Boyce, M. E. C., Argon, A. S. and Parks, D. M., to be published
29 Gebizlioglu, O. S., Argon, A. S. and Cohen, R. E. *Polymer* 1985, **26**, 529